IOPscience iopscience.iop.org

Home Search Collections Journals About Contact us My IOPscience

Detecting measurement-induced relative-position localization

This article has been downloaded from IOPscience. Please scroll down to see the full text article.

2013 J. Phys. B: At. Mol. Opt. Phys. 46 095501

(http://iopscience.iop.org/0953-4075/46/9/095501)

View the table of contents for this issue, or go to the journal homepage for more

Download details:
IP Address: 129.11.69.175
The article was downloaded on 25/04/2013 at 09:45

Please note that terms and conditions apply.

J. Phys. B: At. Mol. Opt. Phys. **46** (2013) 095501 (6pp) doi:10.1088/0953-4075/46/9/095501

Detecting measurement-induced relative-position localization

P A Knott, J Sindt and J A Dunningham

School of Physics and Astronomy, University of Leeds, Leeds LS2 9JT, UK

E-mail: phy5pak@leeds.ac.uk

Received 22 January 2013, in final form 12 March 2013
Published 24 April 2013
Online at stacks.iop.org/JPhysB/46/095501

Abstract
The theory of decoherence explains how classicality emerges from an underlying quantum reality. An additional interpretation to this has been proposed in which scattering events induce the localization of *relative* observables (Rau *et al* 2003 *Science* **301** 1081). An interesting consequence of this process is that it involves the build-up of certain robust entanglements between the observables being localized. To date the weakness of this interpretation has been the lack of a clear experimental signature that allows it to be tested. Here we provide a simple experimentally accessible scheme that enables just that. We also discuss a Bayesian technique that could, in principle, allow experiments to confirm the localization to any desired degree of accuracy and we present precision requirements that are achievable with current experiments. Finally, we extend the scheme from its initial one dimensional proof of principle to the more real world scenario of three dimensional localization.

(Some figures may appear in colour only in the online journal)

1. Introduction

The boundary between quantum and classical physics has long been a perplexing issue for physicists. Why should one set of rules apply to one size scale and another set of rules apparently apply to another? More vexing perhaps is the fact that the boundary that distinguishes the two sets of rules is not sharp, so it is not always clear which theory should be applied.

A lot of work has been done to understand this boundary [2–7] and the prevailing view is that it can be interpreted in terms of decoherence [8–14]. Simply put, this says that quantum systems tend to interact with their environments and become entangled with them. The total system including the environment is therefore properly treated with quantum physics. However, if we are interested only in the quantum subsystem and make measurements only on this, we effectively throw away the information about which environmental states are correlated with which subsystem states. We then find that the subsystem appears to behave more and more classically the more it has interacted with the environment. In effect, by throwing away information about the quantum correlations we are left with a system that behaves classically.

Another interpretation that extends this idea was put forward a few years ago [1, 15]. It showed the emergence of classicality for relative observables, and it does not require us to throw away all the information about the quantum correlations. This is an appealing view since it takes into account the fact that all reference frames are ultimately relative. Furthermore, in this interpretation, even classical objects are entangled with one another but with a special type of robust entanglement sometimes called 'fluffy-bunny' entanglement [16, 17]. This application of quantum theory is attractive as it gives one consistent theory that describes both quantum and classical systems. It is also intriguing that here the emergence of classicality involves entanglement, which is usually thought of as a purely quantum feature.

Despite all the pleasing features of this formalism, up until now it has suffered from the major flaw that it has not been at all clear how it could be tested experimentally. In this paper we resolve this issue by providing a simple, experimentally accessible scheme that could clearly demonstrate this process. This brings the idea into the realm of a testable physical theory. We begin by reviewing the scheme [1] for measurement-induced relative-position localization through entanglement. We then describe the experimental scheme that presents a signature for detecting this process. We finish by showing how the localization can be extended to particles in three dimensions.

 © 2013 IOP Publishing Ltd Printed in the UK & the USA

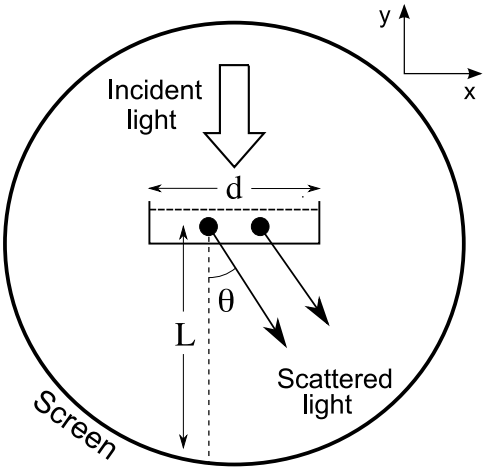

Figure 1. A schematic showing the setup. Two massive particles are delocalized over some region d and are illuminated by plane wave incident light. The scattered light is detected at an angle θ on a screen located at a distance L away from the particles. For clarity, the diagram is not to scale: we consider the case where $L \gg d$.

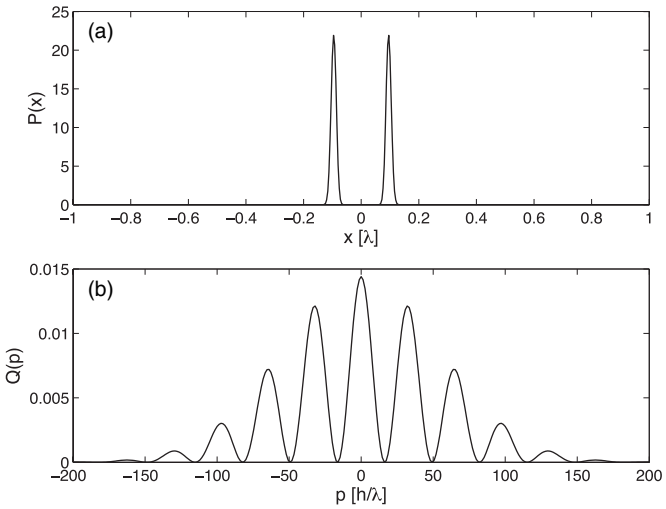

Figure 2. The case of light scattering causing relative localization. (a) Probability density, $P(x)$, for the relative position of the particles after the scattering and detection of 150 photons. The position is given in units of the wavelength, λ, of the scattered light. (b) Probability density, $Q(p)$ for the corresponding relative momentum of the particles.

2. Localization in one dimension

The setup is shown in figure 1. Two particles are delocalized over some region d in the x-direction in the sense that their de Broglie wavelengths are comparable to d in this dimension. We consider the case of distinguishable massive non-interacting particles that are tightly confined in the y and z directions. These two particles will form the sub-systems of the system we are interested in. They are illuminated with plane-wave light with wavelength λ incident along the y-axis, which scatters from them and is detected at an angle θ on a screen located at a distance L away. We will consider the far-field limit where $L \gg d$. The photons are the environmental states of our scheme.

The initial wave function of the particles is $c(x)$ where x represents the *relative* position of the two particles. Since the particles are delocalized over d, the position of one particle relative to the other lies in the range $[-d, d]$. Strictly, to give a full spatial description of the system we should specify the centre-of-mass position as well as the relative position. However the centre-of-mass remains unentangled from the relative position coordinate throughout the scattering process and so can be conveniently neglected [1]. When a photon of wavelength λ scatters off a particle into angle θ, the particle receives a momentum kick in the x-direction of $\Delta p = h \sin\theta/\lambda$, where h is Planck's constant. In relative momentum space the particles therefore receive a kick of $\pm h \sin\theta/\lambda$ depending on which particle the photon scatters from and, since we do not know, we get a superposition of both possibilities. This allows us to write the overall wavefunction of the system after a photon has scattered as:

$$\Psi(x,\theta) = \begin{cases} \frac{1}{2\sqrt{2\pi}} c(x) \left(e^{\frac{i2\pi x}{\lambda}\sin\theta} + e^{\frac{-i2\pi x}{\lambda}\sin\theta} \right) & \text{if } \theta \neq 0 \\ c(x)A(x) & \text{if } \theta = 0 \end{cases}. \quad (1)$$

The probability density for detecting a scattered photon at angle $\theta \neq 0$, and the probability density of detecting a nonscattered photon, $\theta = 0$, are given by:

$$P_S(\theta) = \frac{1}{2\pi} \int_{-d}^{d} |c(x)|^2 \cos^2\left(\frac{2\pi x}{\lambda}\sin\theta\right) \mathrm{d}x \quad (2)$$

$$P_{\mathrm{NS}} = 1 - \int_0^{2\pi} P_s(\theta)\,\mathrm{d}\theta = \int_{-d}^{d} |c(x)|^2 A^2 \mathrm{d}x. \quad (3)$$

From these probabilities, we can deduce:

$$A(x) = \left[\frac{1}{2\pi} \int_0^{2\pi} \sin^2\left(\frac{2\pi x}{\lambda}\sin\theta'\right) \mathrm{d}\theta' \right]^{1/2}. \quad (4)$$

This term represents a nonscattering event that leaves the photon in the undeflected state. It is necessary because the total rate of scattering (integrated over all angles) depends on the separation of the particles, x. Odd as it seems at first sight, this means that detecting a photon that is not scattered gives us information about the relative position of the particles. The $A(x)$ term is required to properly account for this.

To model a scattering event we generate a random number to see whether the photon is scattered and, if so, at what angle. If it is not scattered the (unnormalized) new state is $c(x)A(x)$ and if it is scattered at an angle θ_1, the (unnormalized) new state is given by:

$$\psi(x,\theta_1) = c(x)\cos\left(\frac{2\pi x}{\lambda}\sin\theta_1\right).$$

We then normalize the state and repeat for the next photon.

We choose to start our simulations with a flat distribution, $c(x) = 1/\sqrt{2d}$ because we want to choose the 'hardest' case and show that relative localization builds up even when there is none to begin with. The probability distribution, $P(x)$, for the relative position of the two particles is shown in figure 2(a) for a typical run after 150 photons have been detected and for

$d = \lambda$. We assume that the 150 photons are all incident on the particles in a sufficiently short time period that we do not need to consider the dynamics of the particles between detection events. Initially the distribution is completely flat and we see that the measurement process has induced localization. We have checked the variance of each of the peaks in figure 2(a) and have shown that it varies inversely with the number of scattered photons.

As mentioned above we choose to start our simulations with a flat distribution, but this choice does not restrict the generality of the results and qualitatively similar outcomes are obtained for different choices. For example, we have considered other trap shapes such as harmonic potentials, and found that the trap geometry does not fundamentally affect the results. The light scattering causes relative-position localization regardless of the initial state. As regards to the actual trap used to contain the particles, to highlight the generality of our scheme we have not specified any particular experimental realization. The choice of trap will depend of course on what particles are being used. For example, if we consider atoms there is a broad literature on different trapping techniques such as magneto-optic traps (MOTs) [18, 19].

The above analysis is for monochromatic light of wavelength λ. We have also simulated the localization process for ambient light. For each scattering event the wavelength of the photon is selected from a blackbody distribution. We have used several different temperature blackbody distributions, and we find that in all cases the relative position localization takes place.

3. Proposed experiment to test the localization

The distribution shown in figure 2(a) after 150 photons have been detected has two peaks that are symmetric about the origin. This is what we would expect since we have an equal superposition of either particle being to the 'left'. If the two particles had a well-defined relative position to begin with, then there would be only one peak in this distribution as shown, for example, in figure 3(a). Strictly, in this case we have a mixture of the two different relative positions. This mixture reflects the classical uncertainty in our knowledge of the relative position of the particles based on detecting the scattered photons. The case where the particles are initially delocalized is quite different and gives a coherent superposition of the two relative positions.

The relative-position localization process is analogous to the build-up of relative phase between two number state Bose–Einstein condensates when interference patterns are detected between them [20–22]. Just like in that case we cannot distinguish from the detected photons whether the position (or phase of the BECs) was well-defined to begin with or created by the measurements. We need a way of doing this in order to experimentally verify that the localization process takes place. Although the distinction between figure 2(a) and figure 3(a) is clear, an experimentalist would not have direct access to this since the detected photons cannot tell these distributions apart. One possible solution is to look in the conjugate space—in this case relative momentum. A similar idea has been applied to BECs [23–25].

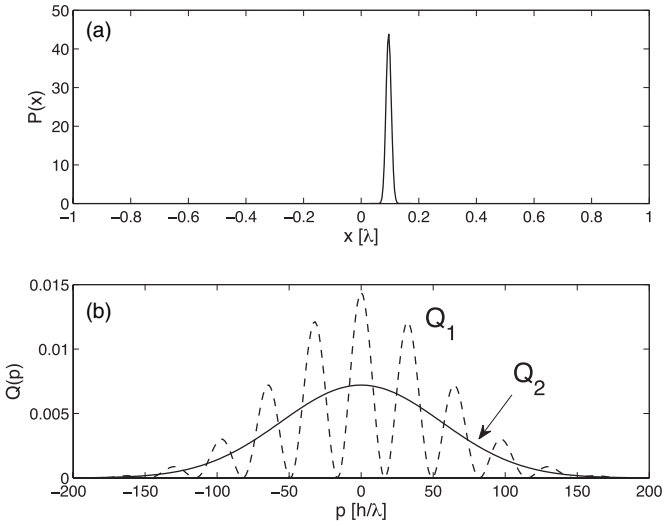

Figure 3. The same as in figure 2 but with the particles initially localized before the photons are scattered. (a) There is now only one peak in the relative position or, strictly, an equally weighted mixture of the two peaks, both of which give the same relative momentum distribution. (b) The corresponding relative momentum probability density is shown as a solid line (labelled Q_2) and is compared to the result in figure 2 shown as a dashed line (labelled Q_1).

The relative momentum distributions corresponding to the relative position distributions in figures 2(a) and 3(a) are shown as the solid lines in figures 2(b) and 3(b) respectively. For ease of comparison, the result from figure 2(b) is superimposed on figure 3(b) as a dashed line. We see that the two distributions have the same envelope, but the case where localization is induced has interference fringes. For particles that are *a priori* perfectly localized, the distribution in figure 3(a) would be a delta function and the momentum distribution would be completely flat. We have chosen the relative position distribution shown because it is an upper limit to the width possible based on the photons detected. In other words, it is the 'hardest' case to distinguish from that shown in figure 2(a). We want to demonstrate that our technique works even in this worst-case scenario.

The measurement scheme is then quite straightforward. After scattering the photons from the particles, we want to distinguish the two relative momentum distributions shown in figure 3(b). To do this, we switch off any trapping potential and allow the particles to move freely. By detecting their positions in the x-direction after some time of flight, we can infer the x-components of their momenta and hence the relative momentum of the particles in that direction. By repeating the whole process from the beginning many times, we should be able to build up a probability distribution and so distinguish the two cases. However, the stochastic nature of the process means that the particles localize to a different relative position on each run and so the relative momentum fringes are different each time. If we were to just naïvely add the results from each run, the fringes would wash out. Instead we can use Bayesian analysis to distinguish the two scenarios.

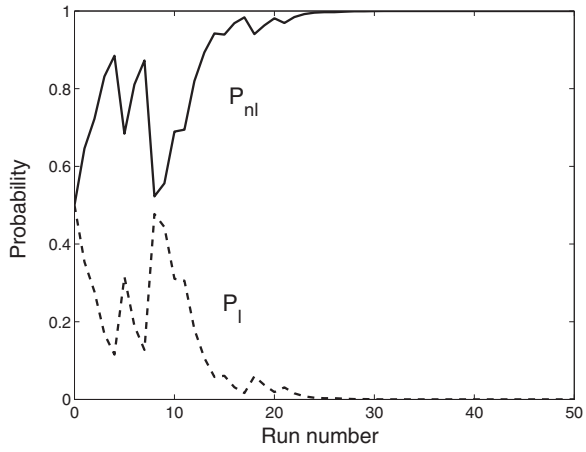

Figure 4. A simulated experiment showing the Bayesian analysis of the probability P_{nl}, that the photon scattering caused relative localization of the particles (solid line) and the probability, P_l, that they were localized to begin with (dashed line). In our simulation, we have taken the particles to start off with no well-defined relative position.

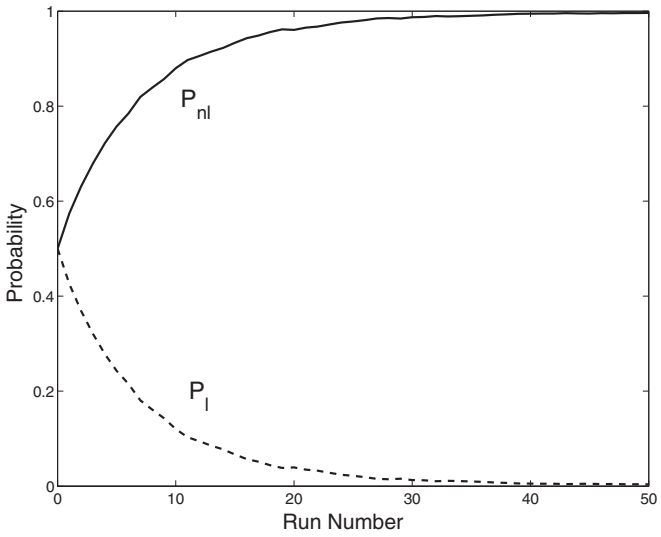

Figure 5. As in figure 4 but averaged over 300 'experiments' to indicate the average number of runs that would be required to achieve a desired degree of confidence.

Suppose on a particular run we detected scattered photons on the screen that meant the relative momentum distribution was either $Q_1(p)$ or $Q_2(p)$ depending on whether or not the scattering process induced relative localization (see figure 3(b)). To begin with, we do not know whether the particles are localized or not so we take our prior probability of them initially being localized, P_l to be the same as the prior probability of them not initially being localized, P_{nl}, i.e. $P_l = P_{nl} = 0.5$. Now suppose, upon releasing the particles, we measure their relative momentum to be p_1. This gives us some information about which scenario is more likely. In particular, Bayes' theorem tells us that the updated probabilities are $P_{nl} \propto Q_1(p_1) \times 0.5$ and $P_l \propto Q_2(p_1) \times 0.5$. Normalizing, we get

$$P_{nl} = \frac{Q_1(p_1)}{Q_1(p_1) + Q_2(p_1)} \times 0.5 \tag{5}$$

and $P_l = 1 - P_{nl}$. We can then iterate this process by using these updated probabilities as the prior probabilities in the next step. By repeating many times we increasingly refine our knowledge of which process is occurring.

A sample simulation is shown in figure 4 for the case that the particles do not initially have a well-defined relative position. We see that initially $P_{nl} = P_l = 0.5$ and that as more and more runs are performed our knowledge of what process is occurring is refined. The probabilities initially jump around for a while before settling down after about 25 runs. The information in this figure is what would be directly accessible to experimentalists and so, in this case, they would be quite certain after about 25 runs that they had observed measurement-induced relative-position localization.

Of course, every experiment would be different due to the stochastic nature of the photon scattering events and the momentum measurements of the particles. So it would be useful to know how many runs on average are likely to be required to achieve a certain degree of confidence. In figure 5 we have averaged the results over 300 simulated experiments. We see that the curves are now quite smooth and that after 20 runs we would expect, on average, to be about 95% confident that measurement-induced relative-position localization is occurring.

So far we have assumed perfect precision of the momentum measurements that allow us to distinguish the two relative momentum distributions shown in figure 3(b). An important question is whether this can still be done when real detectors with imperfect precision are used. To investigate this we convolve the relative momentum probability densities in figure 3(b) with Gaussians of different widths, where each width represents a different resolution of the momentum measurement. We then repeat the above analysis using Bayes' theorem, which gives us the results shown in figure 6. Not surprisingly, it can be seen that as the measurement precision improves, our knowledge about which process has occurred increases more rapidly with the number of runs. In order to be 90% sure that the state was initially delocalized after 20 runs, we need to be able to measure the momentum of the particles with a resolution of $\delta p = 0.5[h/\lambda]$ or less.

As discussed above, we propose that the momentum of the particles is measured by switching off any trapping potential and then detecting the particles' positions in the x-direction after some time of flight. It is the spatial resolution of this position measurement that we are concerned with, and requiring a momentum resolution of $\delta p = 0.5[h/\lambda]$ translates to a detector spatial resolution requirement of approximately 25 μm (this assumes we use Rb-87 atoms, illuminated with violet light, which are allowed to fly for a time of 5 ms along a detector of length 10 mm). Using time-of-flight fluorescence imaging it is possible to spatially resolve the position of a single atom with resolution close to 1 μm [26], and furthermore, Bücker *et al* achieve single atom detection with efficiency close to unity [27], so our required momentum measurement should be achievable with current techniques.

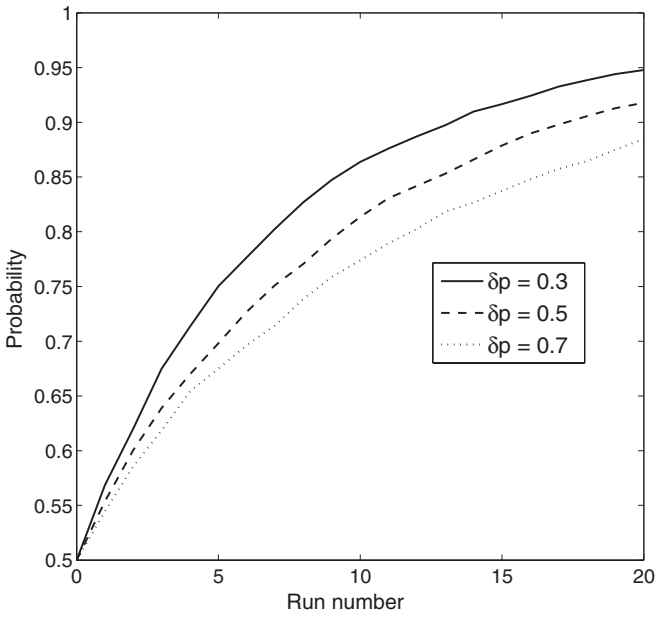

Figure 6. This shows P_{nl}, the probability that photon scattering caused relative localization of the particles, as in figure 5, but here we also include the effect of imperfect measurements. The three different curves show different values of the precision of the momentum measurement: the values of δp here are in units of $[h/\lambda]$. We can see that a resolution of $\delta p = 0.5[h/\lambda]$ is needed for us to be 90% sure that the two particles were initially delocalized after 20 runs have been completed.

4. Extension to three dimensions

We have reviewed a proof of principle for the localization of particles caused by entanglement. We now extend this scheme to particles that are allowed to move in three dimensions. Two distinguishable non-interacting particles are initially delocalized within a 3D cube of length $d = \lambda$. The particles are illuminated with plane-wave light of wavelength λ incident along the z-axis, which scatters from them and is detected at an angle (θ, ϕ) on a spherical screen located at a distance L from the particles, as shown in figure 7. The initial wave function of the particles is $c(x, y, z)$, where x, y and z represent the *relative* position of the two particles in Cartesian coordinates. The wavefunction $c(x, y, z)$ is normalized so that $\int\int\int_D |c(x, y, z)|^2 \, dx\, dy\, dz = 1$, where D represents the box dimensions in which the particles are confined. As in the 1D case, we can neglect the centre-of-mass coordinate of the particles.

We now look at the scattering process: a photon of wavelength λ scatters off a particle into angle (θ, ϕ) in spherical coordinates where θ and ϕ are the polar and azimuthal angles, respectively. A deflected photon will impart the following momentum kick on one of the particles:

$$\Delta p_x = h \sin\theta \cos\phi/\lambda$$
$$\Delta p_y = h \sin\theta \sin\phi/\lambda$$
$$\Delta p_z = h(\cos\theta - 1)/\lambda$$

where h is Planck's constant. In relative momentum space the particles therefore receive a kick of $\pm\Delta p$ where

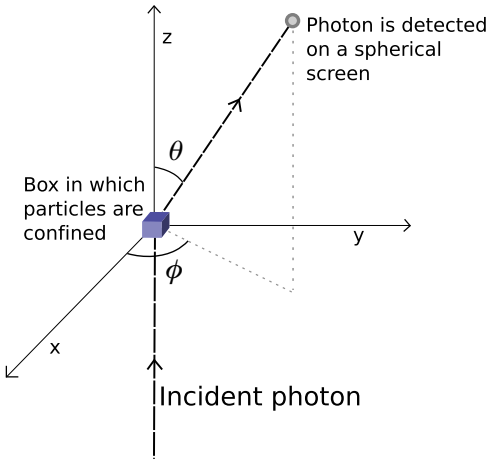

Figure 7. This diagram illustrates the experiment in which two massive particles are delocalized over the volume of a cube with side length d. Plane-wave light with wavelength λ incident along the z-axis scatters from the particles and is detected at an angle (θ, ϕ) on a spherical screen located at a distance L from the particles. For clarity, the diagram is not to scale: we consider the case where $L \gg d$.

$\Delta p = (\Delta p_x, \Delta p_y, \Delta p_z)$. Whether they receive a $+\Delta p$ or $-\Delta p$ kick depends on which particle the photon scatters from, but since this cannot be determined we obtain a superposition of both possibilities.

After one scattering event the overall state of the system is given by:

$$\Psi(x, y, z, \theta, \phi) = \begin{cases} \frac{1}{2\sqrt{\pi}} c(x, y, z) \left(\cos \frac{2\pi}{\lambda} \Gamma_{x,y,z}(\theta, \phi)\right) & \text{if } (\theta, \phi) \neq (0, 0) \\ c(x, y, z) A(x, y, z) & \text{if } (\theta, \phi) = (0, 0) \end{cases} \quad (6)$$

where:

$$\Gamma_{x,y,z}(\theta, \phi) = [x \sin\theta \cos\phi + y \sin\theta \sin\phi + z(\cos\theta - 1)].$$

The probability density for detecting a scattered photon at angle $(\theta, \phi) \neq (0, 0)$ is $P_S(\theta, \phi)$, whereas for a nonscattered photon the probability density is $P_{\mathrm{NS}}(0, 0)$:

$$P_S(\theta, \phi) = \int\int\int_D |\Psi_{(\theta,\phi)\neq 0}|^2 \, dx\, dy\, dz \quad (7)$$

$$P_{\mathrm{NS}} = \int\int\int_D |c(x, y, z)|^2 A^2 \, dx\, dy\, dz. \quad (8)$$

We can then deduce the nonscattering coefficient:

$$A^2(x, y, z) = \frac{1}{4\pi} \int_0^{2\pi} \int_0^{\pi} \sin\theta' \sin^2\left(\frac{2\pi}{\lambda} \Gamma_{x,y,z}(\theta', \phi')\right) d\theta' d\phi'.$$

Again this means that detecting a nonscattered photon can actually give us information about the separation of the particles. The localization process then works in the same way as the 1D case. As before, we generate a random number to see whether the photon is scattered and, if so, at what angle (θ_1, ϕ_1). The (unnormalized) states after the scattering process are as follows, for photons scattered at angle (θ_1, ϕ_1), and non scattered photons, respectively:

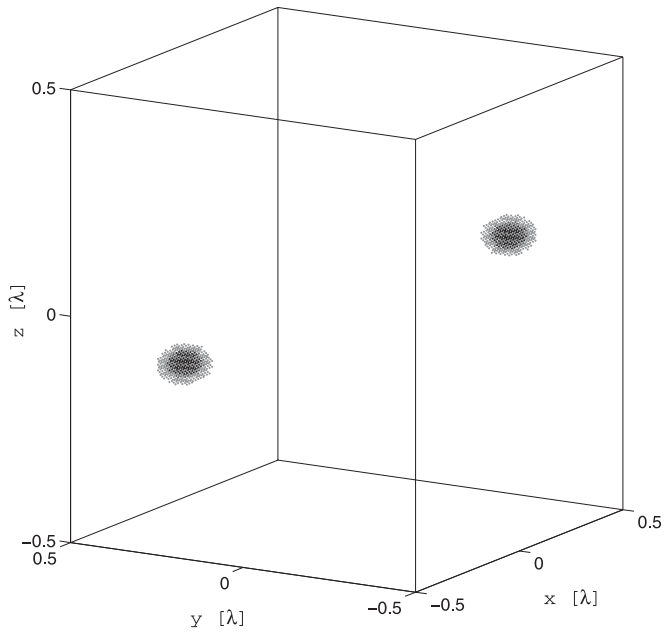

Figure 8. This plot shows the probability density $P(x)$, represented by the density and shading of points, for the relative position of the particles after the scattering and detection of 150 photons. The two high density dark clouds show that as in the 1D case, light scattering has caused relative position localization. The position is given in units of the wavelength, λ, of the scattered light.

$$\Psi_{\theta_1\phi_1} = c(x, y, z) \cos\left(\frac{2\pi}{\lambda}\Gamma_{x,y,z}(\theta_1, \phi_1)\right)$$
$$\Psi_{00} = c(x, y, z)A(x, y, z).$$

We then normalize the state and repeat for the next photon.

We have chosen the initial probability density of the relative positions of the particles to be a flat distribution. We find that after successive photons are scattered off the particles, their relative positions localize, as shown by the probability distribution of the two particles in figure 8 after 150 photons have been scattered. Again we assume that the 150 photons are all incident on the particles in a sufficiently short time period that we do not need to consider the dynamics of the particles between detection events. The high probability density regions in figure 8 are symmetrical about the origin. This reflects the fact that the two particles are interchangeable, and that the localization is a result of successive superpositions of positive and negative relative momentum kicks. This is the desired result: it shows that scattering induced localization can be extended to the more realistic case of particles that are allowed to move in three dimension. As in the one dimensional case, it is important to note that the localization is strictly in *relative* position space: no *absolute* position localization has occurred.

5. Conclusion and discussion

We have demonstrated a simple scheme that should enable experimentalists to unambiguously determine whether scattering events can induce relative position localization for quantum particles. This is an interesting interpretation for how ambient scattering events could lead to the emergence of classical-like behaviour in quantum systems. We have also extended this scheme from a one dimensional proof of principle to the more real world scenario of three dimensions and considered some practical issues for carrying out the experiment. This idea could have important consequences for our understanding of the boundary between quantum and classical physics and the role of relative observables in nature.

Acknowledgment

This work was partly supported by DSTL (contract number DSTLX1000063869).

References

[1] Rau A V, Dunningham J A and Burnett K 2003 *Science* **301** 1081
[2] Zurek W H 1991 *Phys. Today* **44** 36
[3] Zurek W H 2003 *Rev. Mod. Phys.* **75** 715
[4] Schlosshauer M A 2007 *Decoherence and the Quantum-To-Classical Transition* 1st edn (Berlin: Springer)
[5] Bhattacharya T, Habib S and Jacobs K 2003 *Phys. Rev.* A **67** 042103
[6] Ghose S, Alsing P, Deutsch I, Bhattacharya T and Habib S 2004 *Phys. Rev.* A **69** 052116
[7] Everitt M J, Munro W J and Spiller T P 2011 *J. Phys.: Conf. Ser.* **306** 012045
[8] Joos E and Zeh H D 1985 *Z. Phys.* B **59** 223
[9] Ghirardi C G, Rimini A and Weber T 1986 *Phys. Rev.* D **34** 470
[10] Habib S, Shizume K and Zurek W H 1998 *Phys. Rev. Lett.* **80** 4361
[11] Rigo M, Mota-Furtado F and O'Mahony PF 1999 *J. Phys. A: Math. Gen.* **30** 7557
[12] Jacobs K and Steck D A 2011 *New J. Phys.* **13** 013016
[13] Gisin N and Percival I C 1997 arXiv:quant-ph/9701024
[14] Everitt M J 2007 *Phys. Rev.* E **75** 036217
[15] Cable H, Knight P and Rudolph T 2005 *Phys. Rev.* A **71** 042107
[16] Wiseman H M, Bartlett S D and Vaccaro J A 2004 *Laser Spectrosc.* **304**
[17] Dunningham J A, Rau A V and Burnett K 2005 *Science* **307** 872
[18] Phillips W D 1998 *Rev. Mod. Phys.* **70** 721
[19] Wieman C E, Pritchard D E and Wineland D J 1999 *Rev. Mod. Phys.* **71** 253
[20] Javanainen J and Yoo S M 1996 *Phys. Rev. Lett.* **76** 161
[21] Castin Y and Dalibard J 1997 *Phys. Rev.* A **55** 4330
[22] Dunningham J A and Burnett K 1999 *Phys. Rev. Lett.* **82** 3729
[23] Dunningham J A, Burnett K, Roth R and Phillips W D 2006 *New J. Phys.* **8** 182
[24] Mullin W J and Laloë F 2010 *Phys. Rev. Lett.* **104** 150401
[25] Mullin W J and Laloë F 2010 *Phys. Rev.* A **82** 013618
[26] Fuhrmanek A, Lance A M, Tuchendler C, Grangier P, Sortais Y R P and Browaeys A 2010 *New J. Phys.* **12** 053028
[27] Bücker R, Perrin A, Manz S, Betz T, Koller C, Plisson T, Rottmann J, Schumm T and Schmiedmayer J 2009 *New J. Phys.* **11** 103039